IEEE Access
Multidisciplinary | Rapid Review | Open Access Journal

Received June 23, 2021, accepted June 28, 2021, date of publication June 30, 2021, date of current version July 8, 2021.

Digital Object Identifier 10.1109/ACCESS.2021.3093768

The Motion Controller Based on Neural Network S-Plane Model for Fixed-Wing UAVs

PENGYUN CHEN, GUOBING ZHANG, TONG GUAN, MEINI YUAN, AND JIAN SHEN, (Member, IEEE)
College of Mechatronic Engineering, North University of China, Taiyuan 030051, China

Corresponding author: Guobing Zhang (z2831727149@163.com)

This work was supported in part by the National Natural Science Foundation of China under Grant 51909245 and Grant 62003314, in part by the Open Fund of Key Laboratory of High Performance Ship Technology, Ministry of Education, Wuhan University of Technology, under Grant gxnc19051802, in part by the Aeronautical Science Foundation of China under Grant 2019020U0002, in part by the Scientific and Technological Innovation Programs of Higher Education Institutions in Shanxi under Grant 2019L0537, in part by the Natural Science Foundation of Shanxi Province under Grant 201901D211244, and in part by the Open Foundation of Key Laboratory of Submarine Geosciences, MNR, under Grant KLSG2003.

ABSTRACT Aiming at the attitude control problem of fixed wing UAV, this paper introduces S-plane control, which has good control effect in the field of underwater UAV, into the attitude control of UAV. At the same time, aiming at the problem that the coefficient setting of parameters in S-plane control completely depends on experience and cannot be adjusted adaptively, the radial basis function neural network (RBFNN) is introduced, and a neural network S-plane control model which can realize on-line adaptive adjustment of the coefficient of parameters in S-plane control is proposed. The simulation results based on the data of a certain UAV show that compared with the S-plane control, the proposed neural network S-plane control model has the characteristics of fast response speed, strong anti-interference ability, and strong robustness. In addition, it also has the function of adaptive adjustment, which shows good control performance.

INDEX TERMS Fixed wing UAV, S-plane control, radial basis function neural network (RBFNN), adaptive adjustment.

I. INTRODUCTION

In recent years, with the progress of control, electronic information, materials and other aspects of technology, UAV, a high-tech product, has attracted extensive attention in both military and civil aspects [1]. Compared with the manned aircraft, the fixed wing UAV has the characteristics of low cost, zero casualties, reusable, flexible and strong battlefield survivability. The fixed wing UAV is not only used in enemy reconnaissance, ground attack, bee colony operation and target attack, but also plays an important role in agricultural plant protection [2], remote sensing mapping [3], sightseeing photography [1], fire rescue and cargo transportation. Compared with rotorcraft, fixed wing UAV has the characteristics of fast flight speed, large carrying capacity, large cruise radius and good economy [4]. The control system is the brain of UAV, and its performance directly determines the performance of UAV. The control of the rotorcraft is relatively simple, and the fixed wing UAV has higher requirements for the performance of its control system because of the difficulty of operation, which also puts forward higher requirements for the design level and control accuracy of the fixed wing UAV.

The control methods of fixed wing UAV mainly include PID control [2], [5], robust control and other linear control methods, as well as sliding mode control [6], [7], fuzzy control [8], Intelligent control [9], [10] and other nonlinear control methods. Zheng *et al.* [11] Introduced the sliding mode control into the landing control of fixed wing UAV, and combined adaptive control and sliding mode control to compensate the uncertainty of system. Melkou *et al.* [12] Proposed an adaptive second order sliding mode controller, which can reduce the chattering problem in sliding mode. Lungu [13] applies backstep-ping and dynamic backstepping technology to the motion control of fixed wing UAV to suppress the errors caused by wind and sensors during landing. The above control methods all show good control performance, but they all

The associate editor coordinating the review of this manuscript and approving it for publication was Guillermo Valencia-Palomo.

have some problems, such as complicated controller design, difficult application in practice and so on. The S-plane control method, which was invented by Professor Liu Xuemin of Harbin University of engineering, has the characteristics of simple structure, easy parameter adjustment and good control effect [14]. S-plane control is a kind of controller obtained by nonlinear fitting method on the basis of fuzzy control rule table. It has been widely used in underwater unmanned vehicle (UUV). However, the marine environment is usually harsh. Like the fixed wing UAV, the Underwater Unmanned Aerial Vehicle (UUV) also has the characteristics of strong nonlinearity and strong coupling. The key problems of UAV and UUV are similar, so the S-plane control with good control effect in UUA can be introduced into the motion control of UAV. In recent years, S-plane control has also achieved many results. Zhao *et al.* [15] introduced robust control into S-plane control to improve its control performance, however the adjustment of parameters in S-plane still depends on experience. Li, ye *et al* introduce an adaptive term in S-plane control to resist environmental interference. Although it has some practical value, it increases the complexity of structure [16]. Zheng Chen *et al* aimed at the design of the controller faces certain challenging problems in the Multilateral telerobotic system under time delays, various uncertainties, and external disturbance. an adaptive sliding control method based on radial basis function neural network is introduced. which has good position tracking and force feedback performance [17]. Aiming at the robustness and anti-interference of eight rotor UAV, Cheng Peng *et al* Proposed a robust feedback sliding control method by combining the advantages of feedback control and sliding control, and introduced radial basis function neural network as uncertainty observer to improve the robustness of the system [18]. Cao *et al.* [19] aiming at the problem of UAV fault detection, designed a robust adaptive observer based on radial basis function neural network. In this paper, radial basis function neural network is also introduced to solve the problem that the coefficients of parameters in S-plane control cannot be adaptive. Fuzzy control and optimal control have certain ad-vantages in parameter self-tuning, however S-plane control is designed based on fuzzy rule table, which has certain fuzzy characteristics, and the selection of membership function in fuzzy control has certain difficulty. Optimal control is to make the satisfied characteristics reach the maximum or minimum under certain constraints. The UAV motion in this paper needs to adjust the relevant parameters from time to time according to the external environment. In addition, the optimal parameter adjustment is often for a certain period of time or local, the control step size is too small will affect the accuracy. RBFNN has good generalization ability, identification and fault tolerant performance, therefore, it can be used to adjust the S-plane parameters.

In this paper, the S-plane control which has good underwater control effect is introduced into the attitude control of fixed wing UAV. Aiming at the problem that the coefficients of its parameters can not be adaptive, the RBFNN is introduced into the S-plane control, and the RBFNN S-plane control model is created, Then, the corresponding simulation experiments are carried out.

II. STATE EQUATION OF FIXED WING UAV

Suppose that the UAV is a rigid body, the center of gravity of the UAV is set as the origin of the body coordinate system, the ground coordinate system as the inertial system, and the body coordinate system as the moving coordinate system. The connection between them is shown in Fig.1.

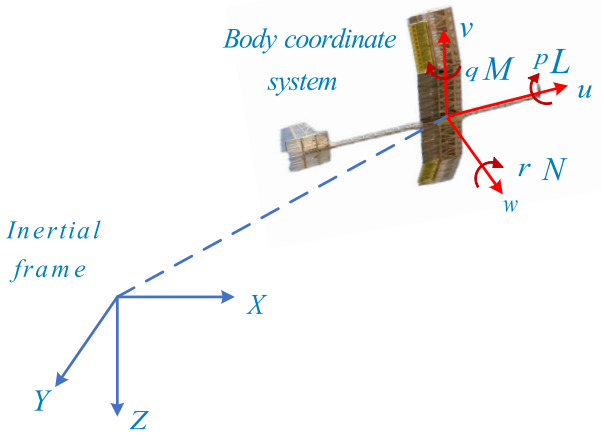

FIGURE 1. UAV model and coordinate system.

The 6-DOF dynamic and kinematic equations of UAV established by Newton's second law [20] are shown in formula (1) (2) (3) (4).

$$\dot{V} = (L + T - D)/m + R(:1) - \omega \times V \tag{1}$$

$$\dot{\Theta} = R' \cdot \omega \tag{2}$$

$$M' = I \cdot \dot{\omega} + \omega \times I \cdot \omega \tag{3}$$

$$\dot{X} = R \cdot V \tag{4}$$

In the formula, $V = [u\ \mathrm{v}\ \mathrm{w}]^T$ represents the linear velocity of the body relative to the inertial system, u, v, w represents the component of linear velocity along x, y and z axes respectively. L is lift, T is thrust, D is resistance; $\omega = [p\ \mathrm{q}\ \mathrm{r}]^T$ represents the angular velocity of the body relative to the inertial system, p, q, r is the component of angular velocity along x, y and z axes; $\Theta = [\phi\ \theta\ \psi]^T$ is the attitude angle of the body, ϕ, θ and ψ represent roll angle, pitch angle and yaw angle respectively; $M' = [L\ \mathrm{M}\ \mathrm{T}]^T$ is the moment on the body. L, M and N represents rolling moment, pitching moment and yaw moment respectively; $X = [x_g\ \mathrm{y}_g\ \mathrm{h}]^T$ is the displacement of the body relative to the inertial coordinate system. Among them, the matrices R', I and R are shown at the bottom of the next page.

In terms of formula (1) (2) (3) (4), It can be decoupled into longitudinal motion equation and lateral motion equation under the assumption that the aircraft is flying horizontally without sideslip. Then, the corresponding longitudinal and lateral state equations are obtained and used as the controlled object. This paper mainly discusses the response of aircraft

longitudinal and lateral parameters under the control of neural network s-plane. The equation of state for longitudinal motion is as follows.

$$\begin{cases} \dot{x} = Ax + Bu \\ y = Cx + Du \end{cases} \tag{5}$$

where x is the state vector, u is the input column vector, y is the output column vector, A is the state transition matrix, B is the control matrix, C is the output matrix, D is the feedforward matrix. Where A and B matrices are expressed as follows:

$$A = \begin{bmatrix} X_u & X_\omega & 0 & X_\theta \\ Z_u & Z_\omega & Z_q & Z_\theta \\ M_u & M_\omega & M_q & 0 \\ 0 & 0 & 1 & 0 \end{bmatrix} B = \begin{bmatrix} X_{\delta_p} & X_{\delta_e} \\ Z_{\delta_p} & Z_{\delta_e} \\ M_{\delta_p} & M_{\delta_e} \\ 0 & 0 \end{bmatrix}$$

The state vector is $x = [\Delta u\ \Delta\omega\ \Delta q\ \Delta\theta]^T$,the input vector is $u = [\Delta\delta_p\ \Delta\delta_e]^T$,the derivation and meaning of other formulas are shown in reference [21]. The state equation of UAV lateral motion is the same as equation (5), the matrix corresponding to A' and B' is as follows:

$$A' = \begin{bmatrix} Y_v & Y_p & Y_\phi & Y_r \\ L_v & L_p & 0 & L_r \\ 0 & 1 & 0 & 0 \\ N_v & N_P & 0 & N_r \end{bmatrix} B' = \begin{bmatrix} 0 & Y_{\delta_r} \\ L_{\delta_a} & L_{\delta_r} \\ 0 & 0 \\ N_{\delta_a} & N_{\delta_a} \end{bmatrix}$$

The state vector corresponding to the lateral state equation is $x = [\Delta v\ \Delta p\ \Delta\phi\ \Delta r]^T$,the input vector is $u = [\Delta\delta_a\ \ \Delta\delta_r]^T$. The stability of the longitudinal and lateral state equations can be proved by Lyapunov's first method, that is to say, formula (6) is used to determine that the corresponding poles are located in the left half plane of s.

$$W = C(sI - A)^{-1}B \tag{6}$$

III. RBFNN S-PLANE CONTROL MODEL

A. S-PLANE CONTROL

The standard S-plane control model is shown in formula (7):

$$u = \frac{2}{1 + \exp[-(k_1 e + k_2 \dot{e})]} - 1.0 \tag{7}$$

The stability of s-plane control has been proved by Jiang CM *et al*, so it will not be repeated here [22]. The three-dimensional surface diagram of S-plane control model is shown in Fig.2 In standard S-plane control, e and $\dot{e}$ represent the normalized control deviation and the change rate of control deviation respectively. k_1 and k_2 are the coefficients of deviation e and deviation change rate $\dot{e}$ respectively. u is the control output. The S-plane control is similar to the proportional differential (PD) control in structure. The adjustment of k_1 and k_2 in S-plane control can be realized by referring to the respective coefficient adjustment of the proportional and differential terms in the PD control. PD control is a linear system, the coefficients of its proportion and integration are fixed, so it is not adaptive. The S-plane control is a non-linear system, which is very suitable for UAV's strongly nonlinear motion control system. But compared with PD control, k_1 and k_2 of S-plane control do not have the function of adaptive adjustment, RBFNN has the function of self-learning and self-adaptive. Therefore, the control mode of RBF with self-adaptive function can be introduced into the S-plane to adjust k_1 and k_2.so that S-plane control has the ability of self-adaptive, and improve the anti-interference ability and control accuracy of the system as much as possible.

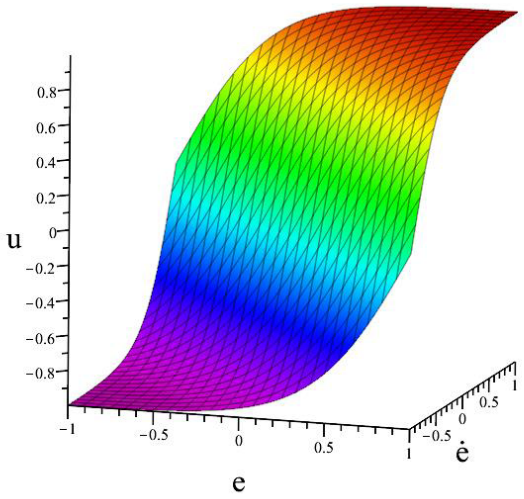

FIGURE 2. 3D surface of S-plane controller.

B. IMPROVEMENT OF S-PLANE CONTROL

As mentioned above, the S-plane control has good control accuracy, but in order to eliminate the influence of the external environment on the control system in flight, the interference adjustment parameter is introduced into the S-plane

$$R' = \begin{bmatrix} 1 & \sin\phi\tan\theta & \cos\phi\tan\theta \\ 0 & \cos\phi & -\sin\phi \\ 0 & \dfrac{\sin\phi}{\cos\theta} & \dfrac{\cos\phi}{\cos\theta} \end{bmatrix} I = \begin{bmatrix} I_x & 0 & I_{xz} \\ 0 & I_y & 0 \\ I_{zx} & 0 & I_z \end{bmatrix}$$

$$R = \begin{bmatrix} \cos\theta\cos\psi & \sin\phi\sin\theta\cos\psi & \cos\phi\sin\theta\cos\psi \\ & -\cos\phi\sin\psi & +\sin\phi\sin\psi \\ \cos\theta\sin\psi & \sin\phi\sin\theta\sin\psi & \cos\phi\sin\theta\sin\psi \\ & +\cos\phi\cos\psi & -\sin\phi\cos\psi \\ \sin\theta & -\sin\phi\cos\theta & -\cos\phi\cos\theta \end{bmatrix}$$

model. In addition, the output range of S-plane control is [-1,1]. In order to improve the control effect, gain needs to be introduced. The final output of S-plane control system is $U = k \cdot u$ at this time, the S-plane control model becomes formula (8);

$$u = k \cdot \left(\frac{2}{1 + \exp[-(k_1 e + k_2 \dot{e})]} - 1.0 + \Delta u \right) \tag{8}$$

at this time, the S-plane control not only has a certain anti-interference ability, but also increases the response strength because of the increase of output gain, which makes the control accurate and fast.

Where Δu is an adjustment item for adapting to environmental interference, it can be written as:

$$\begin{cases} \Delta f = S(\Delta e, 0) \\ \Delta e = (1 - \lambda) e_t + \frac{1}{n} \lambda \beta_t \sum_{i=t-n}^{t} e_i \end{cases} \tag{9}$$

where $S(,)$ denotes the function of S-plane control, e_t is the error at time t, Δe denotes the adaptively adjusted value of error, β_t is the fast weakening factor, λ is the low-pass filter parameter, and n is the number of recorded historical data.in formula (9), the adjustment of β_t is realized by formula (10).

$$\beta_t = \begin{cases} 0.3\beta_{t-1} & \Delta \mathrm{e} \cdot \mathrm{e} < 0 \\ 1 & \text{others} \end{cases} \tag{10}$$

The rapidly weakened part can avoid the error caused by integral lag, The low-pass filter and S-plane control function can adaptive the interference of environment part [16].

C. RBF NEURAL NETWORK

In terms of BP and RBF neural networks. they have their own characteristics. (1) viewed from the structure, The number of layers of BP neural network is at least three, which means that it needs more layers than RBF to solve the problem. In addition, BP neural network input layer and hidden layer, hidden layer and hidden layer, and hidden layer and output layer need to adjust the weight between each node. Every time the data is input, a lot of weights need to be adjusted, which greatly increases the calculation amount. The RBF neural network has only three-layer structure, and the linear relationship between the input layer and the hidden layer only plays the role of data transmission. The hidden layer and the output layer are adjusted by the weight, so the calculation speed is fast. (2) viewed from the function form, the kernel function of BP neural network uses sigmoid function, which will respond to every input value, and has a lot of calculation data, which is a global approximation. The kernel function of RBF neural network is Gauss function, which can only respond to a certain part of the input, so the computation is small and belongs to local approximation. In this paper, we hope that the selected neural network can not only adjust the parameters from time to time, but also operate faster. The RBF neural network can meet this requirement, so we choose the radial basis function neural network to adjust the parameters. at the same time, it also has good generalization ability. Therefore, we choose RBF neural network to design the controller. RBFNN is a three-layer forward feed-back network with a single hidden layer with a local ap-approximation. It has the characteristics of simple structure and fast learning convergence speed. It can convert some low-dimensional input data into high-dimensional space, making the problem of linear inseparability in low-dimensional space is linearly separable in high-dimensional space. Generally speaking, RBFNN model consists of three layers [23], [24]: input layer, hidden layer and output layer, in which the number of nodes in input layer and output layer is related to the dimension of input and output. The number of nodes in the hidden layer is related to the complexity of the controller designed, and the mapping between input layer and implied layer is nonlinear, and the mapping from hidden layer to output layer is linear. The nonlinear mapping function of the hidden layer is mainly realized by the radial basis function. The commonly used radial basis function is Gaussian function, and its expression is as formula (9).

$$h_j(t) = \exp\left(-\frac{\| x(t) - c_j(t) \|^2}{2b_j^2}\right), j = 1, \cdots, m \tag{11}$$

where $x(t)$ is the input vector, $c_j(t)$ is the center vector of the *jth* node in the hidden layer, b_j is the width of the Gaussian function, m is the number of hidden layer nodes, $\| x(t) - c_j(t) \|$ is the Euclidean distance between $x(t)$ and $c_j(t)$. The input layer only plays the role of data transmission, and does not deal with the input information in any form. The linear mapping between hidden layer and output layer is realized by weighting function, the formula is shown in (10).

$$y_i(t) = \sum_{j=1}^{m} \omega_{ji} h_j(t), i = 1, \cdots, n \tag{12}$$

where ω_{ji} is the connection weight between the *jth* node in the hidden layer and the *ith* node in the output layer, n is the number of output nodes, $y_i(t)$ is the output value of node i. The structure diagram of RBFNN is shown in Fig.3.

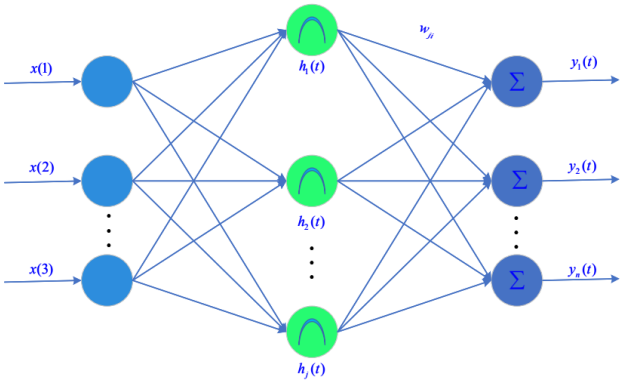

FIGURE 3. Structure diagram of RBFNN.

There are three main parameters to be solved and trained in RBFNN, which are the center of the basis function,

the variance, and the weight from the hidden layer to the output layer. The training process of RBF neural network is divided into two steps: the first step is the unsupervised learning process, which is used to solve the center and variance of the hidden layer basis function. the second step is the supervised learning process, which is used to solve the weights between the hidden layer and the output layer. Before training, the input vector, the corresponding target vector and the learning coefficient need to be provided. The purpose of training is to obtain the final weights and thresholds of the two layers. in the process of unsupervised learning, k- means method is often used to determine the center of basis function. The selection of value in k- means method is difficult, and the selection of initial clustering has a great impact on the results. In addition, the online adaptive method is used to complete the control process, so the center value of the basis function can be determined according to the range of the input function and the density of the data in the Simulink simulation diagram. The variance of the basis function can be obtained by formula (11).

$$b = \frac{c_{\max}}{\sqrt{2j}} \tag{13}$$

where $c_{\max}$ is the maximum distance between the center values of the selected basis function, j is the number of center values of the basis function. In the process of supervised learning, due to the parameters in this paper are relatively few, only k_1 and k_2, and the amount of computation is not very large, gradient descent method is used to train corresponding weights, and the objective function of learning is as formula (12).

$$e(t) = \frac{1}{2}(y(t) - y_i(t))^2, i{=}1, \cdots, n \tag{14}$$

The update rule of output weight is as formula (13) and (14)

$$\Delta\omega_{ji}(t) = -\eta\frac{\partial e(t)}{\partial \omega_{ji}} = \eta(y(t) - y_i(t))h_j(t) \tag{15}$$

$$\omega_{ji}(t) = \omega_{ji}(t-1) + \Delta\omega_{ji} + \alpha[\omega_{ji}(t-1) - \omega_{ji}(t-2)] \tag{16}$$

D. RBFNN S-PLANE CONTROL MODEL

The RBFNN S-plane control model is shown in Fig.4. It is composed of RBFNN parameter regulator, S-plane controller, controlled object and compensation module.

The basic principle of the control is as follows: firstly, the system deviation e and the deviation change rate $\dot{e}$ are transmitted to the RBFNN parameter regulator and the S-plane controller simultaneously as inputs. The deviation e and the deviation change rate $\dot{e}$ input to the RBFNN controller is adjusted online under the function of the RBF neural network algorithm to obtain k_1 and k_2 Then k_1 and k_2 complete the control function of the S-plane controller together with the deviation e and the deviation change rate $\dot{e}$ input to the S-plane controller, and transmit the signal to the controlled object. Finally, under the correction of the compensation module, the output response is obtained. At the same time, the output response is fed back to the input signal to participate in the next step of the control process. In the process of signal reciprocating transmission, online adjustment of parameters in S-plane controller is completed, which improves the adaptive ability of parameters and also improves the control precision and intelligent level of UAV. In addition, the structure of RBF neural network regulator in RBFNN S-plane control is shown in Fig.5.

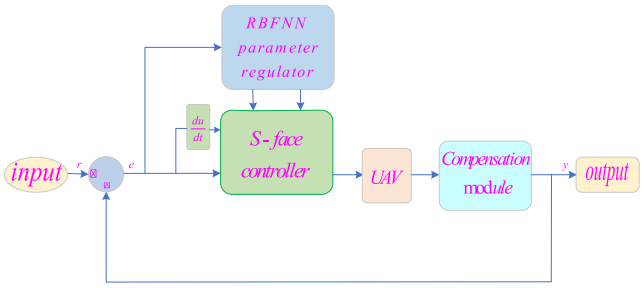

FIGURE 4. Structure diagram of RBFNN S-plane controller.

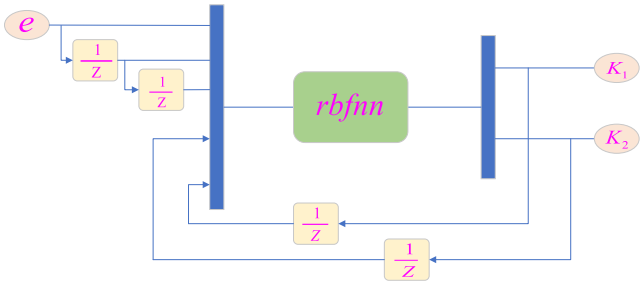

FIGURE 5. Internal structure diagram of RBFNN parameter regulator.

Its input only has deviation e, and the deviation change rate is realized by adding two delays $e(t-1)$ and $e(t-2)$ to the deviation e, and then realized by the form of $(e(t)+e(t-2)-2e(t-1))$ similar to the differential part in the discrete incremental PID control. The function of module RBFNN in Fig.5. is realized by the S-Function function in MATLAB, S-function is aimed at some complex dynamic problems in simulation. When other modules cannot solve them, it realizes the connection with other modules by writing specific functions. It has a fixed format, as shown in formula (15).

$$function[sys, x_0, str, ts] = f(t, x, u, flag, z_1, \cdots) \tag{17}$$

where f is the function name of S-Function, x_0, str, ts represent the initial state vector, description vector and sampling period vector respectively. t, x, u represents time, state vector and input signal respectively. *flag* is the State Flag of function, which is used to judge the current state of Function. When $flag = 0$, S-Function will initialize the function and set some related parameters. When $flag = 1$ and 2, continuous state variables and discrete state variables are updated respectively, and the updated state variable is returned through *sys*. When $flag = 3$, the output of the

system is obtained through *mdloutputs*() function and the output signal is returned through *sys*. When *flag* = 4, the next simulation time is calculated and returned by *sys*. When *flag* = 9, the simulation terminates without returning any variables. In the simulation, *flag* = 0 is executed to initialize. Then the output is calculated by *flag* = 3. At the end of the simulation cycle, let *flag* = 1 or 2, update the continuous or discrete variables of the system, and then execute the *flag* = 3 operation, so as to cycle back and forth until *flag* = 9.

E. RBFNN PARAMETER REGULATO OPTIMIZATION

In the RBFNN parameter regulator, the input data are the deviation e and the deviation change rate $\dot{e}$, which are generally small. The Gauss function in the hidden layer of the RBFNN can produce local response to the input signal, that is, the closer the input deviation e and the deviation change rate $\dot{e}$ are to the center of the Gauss basis function, the stronger the response. However, the output of Gauss function is small. In S-plane control, when the input coefficient changes greatly, the response is more intense. Therefore, in order to make the output of RBFNN parameter regulator act better on the S-plane controller and make its control more effective, a gain k_1' and a gain k_2' are added to the output of RBFNN parameter regulator.

IV. EXTERNAL WIND MODELING

According to the characteristics of wind, the modeling of UAV external wind interference can be expressed as the combination of basic wind v_b, gust v_g,random wind v_r and gradual wind v_n as shown in formula (17)

$$V = v_b + v_g + v_r + v_n \tag{18}$$

The basic wind is the average wind speed acting on the UAV, which can be regarded as a constant determined by the formula (18).

$$v_b = k, \ \text{k is a constant} \tag{19}$$

Gust reflects the mutation type of wind, determined by formula (19).

$$v_g \begin{cases} (v_{g\max}/2)[1-\cos(2\pi(t-T_1)/T_g)], & T_1 \le t \le T_1+T_g \\ 0, & \text{other} \end{cases} \tag{20}$$

where, $v_{g\max}$ is the maximum value of gust, T_1 is the gust start time, T_g is the gust period.

The gradual wind reflects the gradual change of the wind speed, determined by formula (20).

$$v_n = \begin{cases} v_{n\max}[(t-T_1')/(T_2'-T_1')], & T_1' \le t \le T_2' \\ v_{n\max}, & T_2' \le t \le T_2'+T \\ 0, \text{ other} \end{cases} \tag{21}$$

where, $v_{n\max}$ is the maximum value of gradual wind, T_1' is the start time of the gradual wind, T_2' is the end time of the gradual wind, T is the period of gradual wind. Random wind reflects the randomness and uncertainty of wind speed. Determined by formula (21).

$$v_r = v_{r\max} r_a(-1, 1)\cos(\gamma + \eta) \tag{22}$$

where, $v_{r\max}$ is the maximum value of random wind, $r_a(-1, 1)$ is a random number uniformly distributed between -1 and 1, γ is the average distance of wind speed fluctuation, the general value is $0.5\pi \sim 2\pi$. η is the random quantity of uniform distribution between $0 \sim 2\pi$.

V. SIMULATION TEST AND RESULT ANALYSIS

A. TYPES OF GRAPHICS

In the simulation, the data of longitudinal and lateral state equations of UAV in literature [25] are used. In the longitudinal equation of state, A and B are respectively:

$$A = \begin{bmatrix} -0.0088 & -0.0105 & 0 & -0.0409 \\ -0.0915 & -0.4917 & 1 & 0 \\ -0.0294 & -2.5464 & -0.8966 & 0 \\ 0 & 0 & 1 & 0 \end{bmatrix}$$

$$B = \begin{bmatrix} 0 \\ -0.1011 \\ -7.7307 \\ 0 \end{bmatrix}$$

In the lateral state equations, A' and B' are respectively:

$$A' = \begin{bmatrix} -0.15008 & 0.11649 & 0.06115 & 1 \\ -26.12497 & -1.65932 & 0 & -1.04318 \\ 0 & 1 & 0 & 0 \\ -3.59812 & -0.06277 & 0 & -0.29365 \end{bmatrix}$$

$$B' = \begin{bmatrix} 0 \\ -1.59378 \\ 0 \\ -0.02872 \end{bmatrix}$$

where $C = [1111], D = [0]$ when the element in C is 1, outputs the result or image of the corresponding element.

B. SIMULATION AND RESULT ANALYSIS

The simulation experiment in this paper is carried out in the Simulink simulation environment of MATLAB. In order to verify the control performance of the designed RBFNN S-plane control, the S-plane control is introduced as the control group for comparison. Firstly, the longitudinal motion of UAV is simulated, the values of A, B, C and D are substituted into the longitudinal state equation in turn, and then the step signal is added to the input signal. The step response of longitudinal motion is shown in Fig.6 Compared with S-plane control in the speed and pitch angle step response, RBFNN S-plane control has the characteristics of fast response, no overshoot, and short transition process time. In the angular rate step response, RBFNN S-plane control changes smoothly and can reach a stable state quickly, showing good control performance. In order to verify the anti-interference ability of RBFNN S-plane control in longitudinal control, Gaussian white noise interference is added in period $20s < t < 40s$

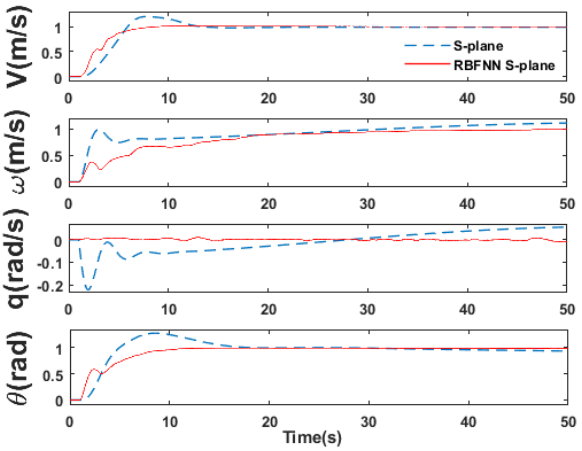

FIGURE 6. Longitudinal step response curve of UAV.

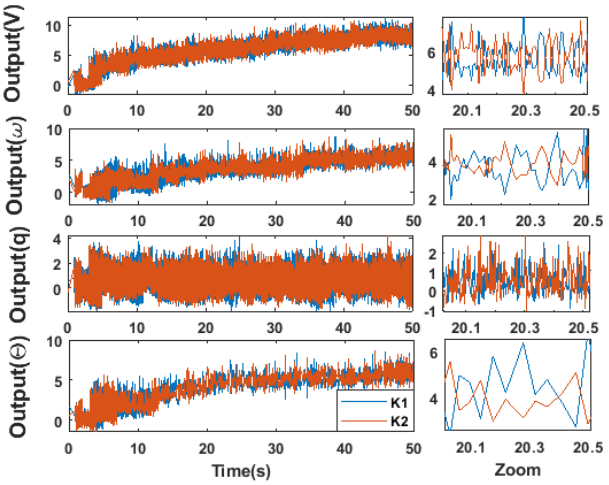

FIGURE 8. Coefficient variation diagram in longitudinal controller.

of step response in Fig.6, and the response result is shown in Fig.7. In the angular rate step interference response, the RBFNN S-plane control and S-plane control responses are relatively strong, however the RBFNN S-plane control still has strong anti-interference ability. Among other parameters of longitudinal motion, the anti-interference capability of RBFNN S-plane control is better than S-plane control. Fig. 8 shows the output result of RBFNN parameter regulator in longitudinal motion, and is also the coefficient of deviation and deviation change rate of S-plane controller in longitudinal motion. It can be seen from Fig.8 that RBFNN S-plane control can realize the constant adjustment of the correlation coefficient in the S-plane controller, showing good robust performance.

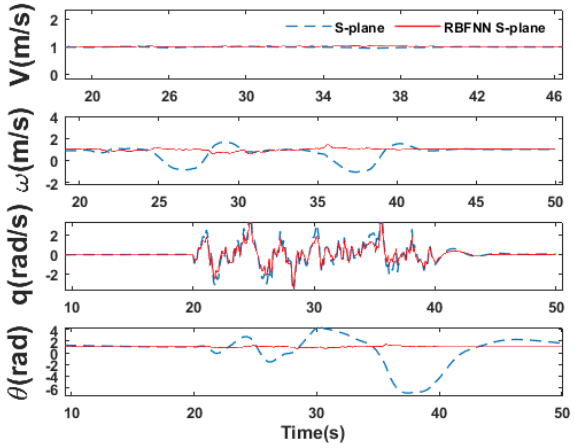

FIGURE 7. Longitudinal interference curve of UAV.

In the lateral movement of the UAV, after inputting the relevant parameters A, B, C and D of the state equation in turn, and then the step signal is added to the input signal. The step response of lateral motion is shown in Fig.9. In the angular rate response along the axis, RBFNN S-plane control responds quickly and can always maintain a stable state. In the angular rate response along the axis, RBFNN S-plane control has stable response and tends to be stable quickly compared with S-plane control. In the roll angle response, RBFNN S-plane response is slow, but its rise time is relatively fast, no vibration, no overshoot, and has good control performance. In order to verify the anti-interference ability of RBFNN S-plane in lateral motion, Gaussian white noise interference is added in period $65s < t < 95s$ of step response in Fig.9, and the response result is shown in Fig.10 in the angular rate interference response along the X axis, the RBFNN S-plane control and S-plane control responses are relatively strong, but RBFNN S-plane has stronger anti-interference ability. In the side-slip angle and angular rate interference response along the Z axis, RBFNN S-plane control is similar to that of S-plane control. But in the roll angle interference response, the anti-interference performance of RBFNN S-plane control is significantly better than S-plane control. Therefore, RBFNN S-plane control has strong anti-interference ability in lateral motion. Fig.11 is

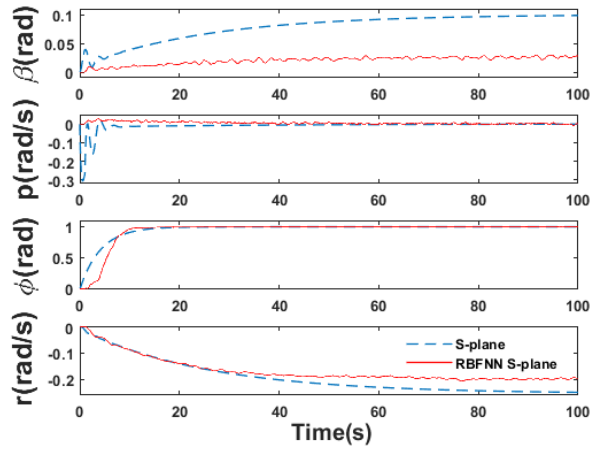

FIGURE 9. Lateral step response curve of UAV.

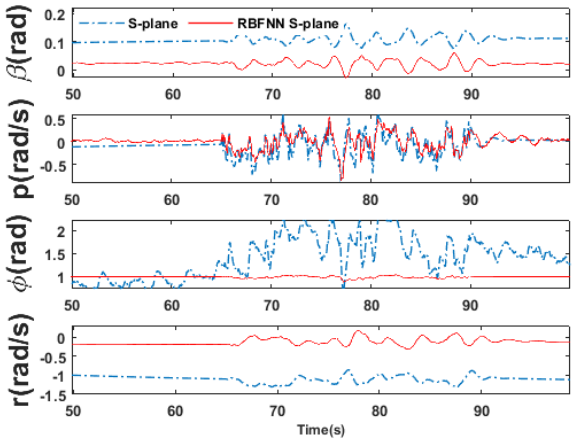

FIGURE 10. Lateral interference curve of UAV.

the output result of the RBFNN S-plane parameter regulator in the lateral movement, and it is also the variation of the coefficients corresponding to the deviation and the deviation change rate in the lateral S-plane. It can be seen from Fig.11 that the coefficients of deviation and deviation change rate can be adjusted from time to time according to the changes of input and external interference to meet different responses.

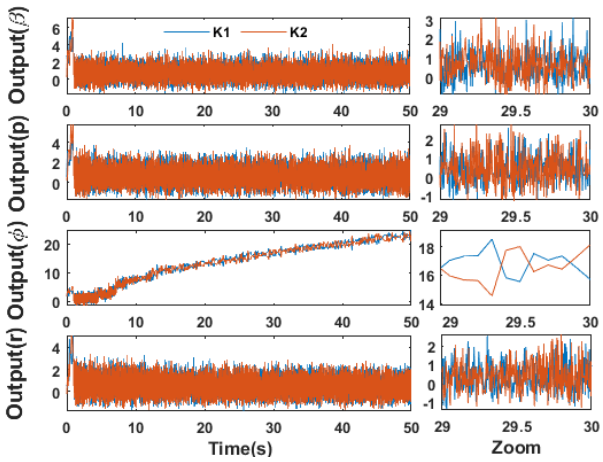

FIGURE 11. Coefficient variation diagram in lateral controller.

Fig.6 and Fig.9 are the response diagrams of UAV longitudinal motion and lateral motion in step input, reflecting the input-output relationship at a certain time. In order to verify the response ability of the designed RBFNN S-plane control in a continuous time period more accurately, The velocity V,pitch angle θ,and roll angle ϕ along y direction is simulated again. The simulation results are shown in Fig.12, In the response of the velocity along the y direction, the input signal is a signal similar to the ladder shape. it can be seen that compared with the S-plane control, the RBFNN S-plane control can track the input signal more quickly and accurately, while the S-plane control has the phenomenon of overshoot and tracking deviation in the rising phase of the ladder signal. Sinusoidal signals are used as input signals in pitch angle and roll angle responses in attitude control. It can be seen from the

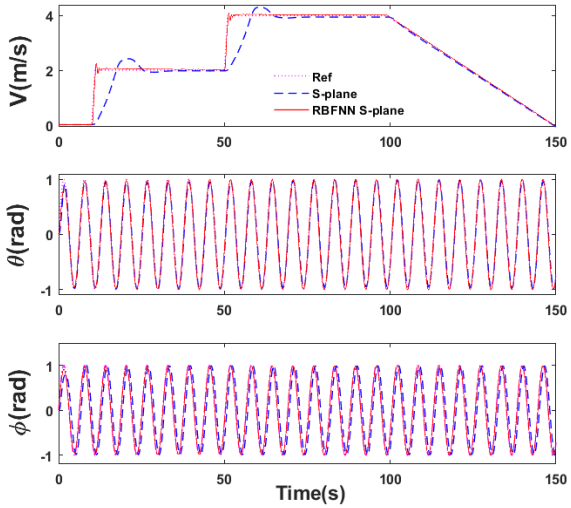

FIGURE 12. Velocity and attitude response diagram.

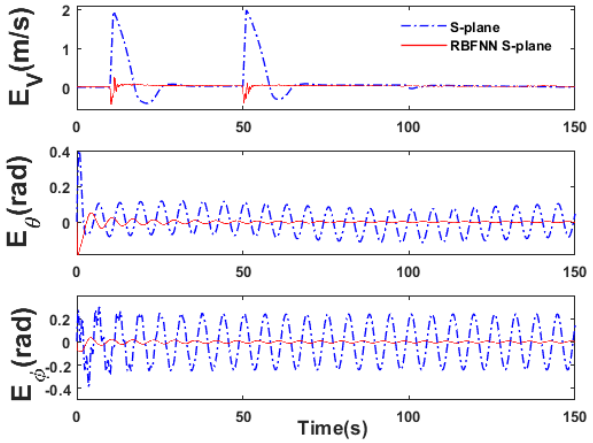

FIGURE 13. Velocity and attitude response error diagram.

simulation results in Fig.12 that RBFNN S-plane control and S-plane control can track the input signal well and respond quickly. In the roll angle response, S-plane control has a slightly delayed response compared with RBFNN S-plane control. Fig.13 is an error diagram of RBFNN S-plane control, S-plane control response and input signal in Fig.12. It can be seen that in the velocity response along the y axis, the error is large when t = 10s and t = 50s. that is, when the step signal rises, the RBFNN S-plane control has good control performance. In the response of pitch angle and roll angle, S-plane control has relatively large error, which also shows that the response of S-plane control is relatively slow compared with RBFNN S-plane control, however, the error of RBFNN S-planed approaches 0 basically. The results show that RBFNN S-plane can track the input signal better, and the response is accurate and fast.

VI. CONCLUSION

In this paper, aiming at the control problem of fixed wing UAV, a simple and practical S-plane control is introduced into the attitude control. Considering that the coefficients of the parameters in the S-plane control do not have adaptive

adjustment, the neural network was introduced, and an RBFNN S-plane control model was designed to improve the accuracy of attitude control in fixed-wing UAVs. after that, under the comparison of S-plane control, the simulation of longitudinal motion and lateral motion verified that the RBFNN S-plane model has good control accuracy. The conclusions are as follows:

(1) The improved S-plane control and the optimized neural network parameter regulator have good control effect in attitude control.

(2) In RBFNN S-plane control, the coefficients of S-plane module parameters have the function of self-adaptive adjustment, which can respond to different inputs at any time and has strong anti-interference ability.

(3) The simulation results show that RBFNN S-plane control has good anti-interference performance and robustness compared with S-plane control, and the error of speed, pitch angle and roll angle in sinusoidal input response is less than 0.1 except for a few individual points. It has high control precision.

REFERENCES

[1] K. Yan, M. Chen, Q. X. Wu, and R. G. Zhu, "Robust adaptive compensation control for unmanned autonomous helicopter with input saturation and actuator faults," *Chin. J. Aeronaut.*, vol. 32, no. 10, pp. 2230–2299, Oct. 2019, doi: 10.1016/j.cja.2019.06.001.

[2] Ş. Ulus and Ł. Eski, "Neural network and fuzzy logic-based hybrid attitude controller designs of a fixed-wing UAV," *Neural Comput. Appl.*, vol. 33, no. 14, pp. 8821–8843, Jan. 2021, doi: 10.1007/s00521-020-05629-5.

[3] A. Panta, A. Mohamed, M. Marino, S. Watkins, and A. Fisher, "Unconventional control solutions for small fixed wing unmanned aircraft," *Prog. Aerosp. Sci.*, vol. 102, pp. 122–135, Oct. 2018, doi: 10.1016/j.paerosci.2018.07.005.

[4] T. Espinoza, A. E. Dzul, R. Lozano, and P. Parada, "Backstepping–sliding mode controllers applied to a fixed-wing UAV," *J. Intell. Robot. Syst.*, vol. 73, nos. 1–4, pp. 67–79, Jan. 2014, doi: 10.1007/s10846-013-9955-y.

[5] T. Espinoza, A. Dzul, and M. Llama, "Linear and nonlinear controllers applied to fixed-wing UAV," *Int. J. Adv. Robot. Syst.*, vol. 10, no. 1, p. 33, Jan. 2013, doi: 10.5772/53616.

[6] A. T. Espinoza-Fraire, Y. Chen, A. Dzul, R. Lozano, and R. Juarez, "Fixed-wing MAV adaptive PD control based on a modified MIT rule with sliding-mode control," *J. Intell. Robot. Syst.*, vol. 91, no. 1, pp. 101–114, Jul. 2018, doi: 10.1007/s10846-018-0856-y.

[7] J. F. Gomez and M. Jamshidi, "Fuzzy adaptive control for a UAV," *J. Intell. Robot. Syst.*, vol. 62, no. 2, pp. 271–293, May 2011, doi: 10.1007/s10846-010-9445-4.

[8] M. M. Ferdaus, S. G. Anavatti, M. Pratama, and M. A. Garratt, "Towards the use of fuzzy logic systems in rotary wing unmanned aerial vehicle: A review," *Artif. Intell. Rev.*, vol. 53, no. 1, pp. 257–290, Jan. 2020, doi: 10.1007/s10462-018-9653-z.

[9] W. Gu, K. P. Valavanis, M. J. Rutherford, and A. Rizzo, "UAV model-based flight control with artificial neural networks: A survey," *J. Intell. Robot. Syst.*, vol. 100, nos. 3–4, pp. 1469–1491, Dec. 2020, doi: 10.1007/s10846-020-01227-8.

[10] E. Kayacan, M. A. Khanesar, J. Rubio-Hervas, and M. Reyhanoglu, "Learning control of fixed-wing unmanned aerial vehicles using fuzzy neural networks," *Int. J. Aerosp. Eng.*, vol. 2017, pp. 1–12, 2017, doi: 10.1155/2017/5402809.

[11] Z. W. Zheng, Z. H. Jin, L. Sun, and M. Zhu, "Adaptive sliding mode relative motion control for autonomous carrier landing of fixed-wing unmanned aerial vehicles," *IEEE Access*, vol. 5, pp. 5556–5565, 2017, doi: 10.1109/ACCESS.2017.2671440.

[12] L. Melkou, M. Hamerlain, and A. Rezoug, "Fixed-wing UAV attitude and altitude control Via adaptive second-order sliding mode," *Arabian J. Sci. Eng.*, vol. 43, no. 12, pp. 6837–6848, Dec. 2018, doi: 10.1007/s13369-017-2881-8.

[13] M. Lungu, "Backstepping and dynamic inversion combined controller for auto-landing of fixed wing UAVs," *Aerosp. Sci. Technol.*, vol. 96, Jan. 2020, Art. no. 105526, doi: 10.1016/j.ast.2019.105526.

[14] X. M. Liu and R. Y. Xu, "S-plane control method for underwater vehicle motion," *Ocean Eng.*, vol. 19, pp. 81–84, Mar. 2001.

[15] X. C. Zhao, M. N. Yuan, P. Y. Cheng, L. Xin, and L. B. Yao, "Robust H_∞ S-plane controller of longitudinal control for UAVs," *IEEE Access*, vol. 7, pp. 91367–91374, 2019, doi: 10.1109/ACCESS.2019.2927000.

[16] Y. Li, L. An, Y. Jiang, J. He, J. Cao, and H. Guo, "Dynamic positioning test for removable of ocean observation platform," *Ocean Eng.*, vol. 153, pp. 112–121, Apr. 2018, doi: 10.1016/j.oceaneng.2018.01.079.

[17] Z. Chen, F. Huang, W. Chen, J. Zhang, W. Sun, J. Chen, J. Gu, and S. Zhu, "RBFNN-based adaptive sliding mode control design for delayed nonlinear multilateral telerobotic system with cooperative manipulation," *IEEE Trans. Ind. Informat.*, vol. 16, no. 2, pp. 1236–1247, Feb. 2020, doi: 10.1109/TII.2019.2927806.

[18] C. Peng, Y. Bai, X. Gong, Q. Gao, C. Zhao, and Y. Tian, "Modeling and robust backstepping sliding mode control with adaptive RBFNN for a novel coaxial eight-rotor UAV," *IEEE/CAA J. Automatica Sinica*, vol. 2, no. 1, pp. 56–64, Jan. 2015, doi: 10.1109/JAS.2015.7032906.

[19] C. Lijia, T. Yu, and Z. Guo, "Adaptive observer-based fault detection and active tolerant control for unmanned aerial vehicles attitude system," *IFAC-PapersOnLine*, vol. 52, no. 24, pp. 47–52, 2019.

[20] H. Castañeda, O. S. Salas-Peña, and J. D. León-Morales, "Extended observer based on adaptive second order sliding mode control for a fixed wing UAV," *ISA Trans.*, vol. 66, pp. 226–232, Jan. 2017, doi: 10.1016/j.isatra.2016.09.013.

[21] S. T. Wu and Y. H. Fei, *Flight Control System*. Beijing, China: Beijing Univ. Aeronautics and Astronautics Press, 2005, pp. 79–101.

[22] C.-M. Jiang, L. Wan, Y.-S. Sun, and Y.-M. Li, "Design of novel sliding-mode controller for high-velocity AUV with consideration of residual dead load," *J. Central South Univ.*, vol. 25, no. 1, pp. 121–130, Jan. 2018, doi: 10.1007/s11771-018-3722-y.

[23] S. Zeghlache, H. Mekki, A. Bouguerra, and A. Djerioui, "Actuator fault tolerant control using adaptive RBFNN fuzzy sliding mode controller for coaxial octorotor UAV," *ISA Trans.*, vol. 80, pp. 267–278, Sep. 2018, doi: 10.1016/j.isatra.2018.06.003.

[24] Y. Song, L. He, D. Zhang, J. Qian, and J. Fu, "Neuroadaptive fault-tolerant control of quadrotor UAVs: A more affordable solution," *IEEE Trans. Neural Netw. Learn. Syst.*, vol. 30, no. 7, pp. 1975–1983, Jul. 2019, doi: 10.1109/TNNLS.2018.2876130.

[25] S. T. Wang, *Design of Flight Control System for Fixed Wing UAV*. Beijing, China: Beijing Univ. Technology, 2015, pp. 42–45.

PENGYUN CHEN received the B.S. and Ph.D. degrees in design and construction of naval architecture and ocean structure from Harbin Engineering University, Harbin, China, in 2010 and 2016, respectively. Since 2016, he has been a Lecturer with the College of Mechatronic Engineering. Since 2020, he has also been an Associate Professor with the North University of China. His research interests include the autonomous control and navigation technology of unmanned vehicle, optical target recognition, and tracking.

GUOBING ZHANG received the B.S. degree in aircraft manufacture engineering from the College of Aeronautics and Astronautics, Shenyang Aerospace University, in 2019. He is currently pursuing the master's degree with the College of Mechatronics Engineering, North University of China. His research interests include UAV attitude control, trajectory tracking, and path planning.

TONG GUAN received the B.S. degree in aircraft design and engineering from the College of Mechatronic Engineering, North University of China, in 2019, where he is currently pursuing the master's degree in flight mechanics and control. The flight control research work is carried out at the UAV Innovation Laboratory, North University of China. He has published one academic articles. His research interests include UAV and control systems.

MEINI YUAN received the Ph.D. degree from Northwestern Polytechnical University, in 2009. She is currently a Professor and a Doctoral Supervisor with the College of Mechatronic Engineering, North University of China. She is in charge of the Doctoral Programs Fund of the Ministry of Education, the Shanxi Natural Resources Fund, the National Natural Science Foundation of China, the National Solidification Key Laboratory Innovation Fund, and the Postdoctoral Fund. She has participated in the completion of Aviation Fund, ''Eleventh Five-Year'' Pre-Research, and the National Natural Science Foundation of China, and a number of projects. She has published more than 30 articles in domestic and foreign journals, and more than 20 articles have been included in SCI and EI. She edited one textbook and one monograph of the 12th Five-Year Plan at the provincial and ministerial level. She had an application for a utility model patent. In recent years, she has been involved in the teaching and research of integrated design of aviation structure, dynamics and control of aircraft structure, and mechanics mechanism of fracture and damage.

JIAN SHEN (Member, IEEE) was born in Shanxi, China, in 1988. He received the B.Sc. degree in electromechanical engineering from the North University of China, Taiyuan, China, in 2010, and the Ph.D. degree from the Beijing Institute of Technology, in 2017. He is currently an Assistant Professor of electromechanical engineering with the North University of China. His current research interests include cooperative control, prognostic, and health management of unmanned aerial vehicle formation.